Proceedings of the
44th IEEE Conference on Decision and Control, and
the European Control Conference 2005
Seville, Spain, December 12-15, 2005

Multivariable PPF Control of an Active Structure

S. O. R. Moheimani, B. J. G. Vautier and B. Bhilkkaji

Abstract— **This paper reports experimental implementation of extended positive position feedback (PPF) controller on an active structure consisting of a cantilevered beam with bonded collocated piezoelectric actuators and sensors. Stability conditions for PPF control are rederived to allow for a feed-through term in the model of the structure which is needed to ensure little perturbation in the in-bandwidth zeros of the model. The set of stabilizing PPF controllers is shown to be a convex set characterized by a set of linear matrix inequalities. A multivariable PPF controller is designed and successfully implemented on the structure.**

I. Introduction

A major difficulty in control of flexible structures is due to the fact that they are distributed parameter systems. Consequently, these structures have a very large number of vibration modes and their transfer functions contain many poles close to the $j\omega$ axis. These systems are generally difficult to control.

Very often a small number of in-bandwidth modes of the structure are required to be controlled, and it is possible that some in-bandwidth modes are not targeted to be controlled at all. The presence of uncontrolled modes can lead to the problem of spillover [1]. That is, the control energy is channeled to the residual modes of the system and this process may destabilize the closed-loop system. In particular, the spillover effect is of major concern at higher frequencies where obtaining a precise model of the structure is rather difficult.

One approach to overcome the spillover effect is based on using collocated sensors and actuators. Positive position feedback as proposed by Caughey and co-authors [5], [4] is a control design technique for flexible structures with collocated sensors and actuators, which is insensitive to spillover effect. The PPF does not guarantee unconditional stability of the closed-loop system, however, it does guarantee stability in presence of uncontrolled in-bandwidth modes, and it has the additional property that it rolls off quickly at higher frequencies.

One of the shortcomings of the PPF as proposed in [5] and [4] is that the effect of out-of-bandwidth modes on the dynamics of the controlled modes is ignored. This effect can be captured by adding a feed-through term to the truncated model of the structure. In this paper we derive stability conditions for PPF controllers when the underlying structure model contains a feed-through term. We also design a multivariable PPF controller for a test structure consisting of a cantilevered beam and several bonded piezoelectric actuators and sensors. Although a drastic simplification of a real structure, a thin beam is dynamically well understood, retains the important characteristics of the real structure and is an ideal experimental testbed to evaluate performance of the PPF controllers.

This research was supported by the Australian Research Council.

School of Electrical Engineering and Computer Science, University of Newcastle, NSW, Australia. Reza.Moheimani@newcastle.edu.au

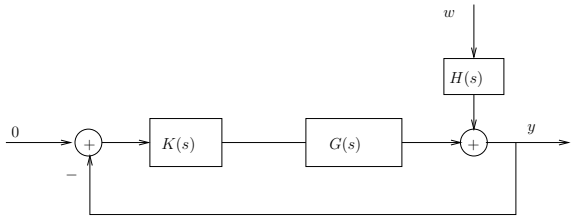

Fig. 1. Feedback control system associated with a flexible structure with collocated actuator/sensor pairs, and subject to disturbance w

II. Resonant systems

In this paper we are concerned with designing high-performance feedback controllers for multivariable resonant systems of the form:

$$G(s) = \sum_{i=1}^{M} \frac{\psi_i \psi_i'}{s^2 + 2\zeta_i \omega_i s + \omega_i^2} \tag{1}$$

where ψ_i is an $m \times 1$ vector, and $M \to \infty$. In practice, however, the integer M is finite, but possibly a very large number which represents the number of modes that sufficiently describe the elastic properties of the structure under excitation [6]. Furthermore, the structure could be subject to disturbances represented by w, whose effect may be captured by a transfer function $H(s)$. This could represent point forces, distributed forces (such as a wind gust) or torques acting on the structure. Nevertheless, the transfer function matrix relating the disturbance vector w to the measured outputs can be represented as

$$H(s) = \sum_{i=1}^{M} \frac{\psi_i \gamma_i'}{s^2 + 2\zeta_i \omega_i s + \omega_i^2} \tag{2}$$

where γ_i is a $\ell \times 1$ matrix, assuming there are ℓ disturbances acting on the structure.

For the SISO case, i.e. when $G(s)$ represents the transfer function associated with only one collocated actuator/sensor pair, this system is known to possess interesting properties [7]. In particular, it is known that the system is minimum phase, and furthermore, poles and zeros of the system interlace. This ensures that phase of the collocated transfer function will be within the 0 to -180° range.

Given the highly resonant nature of flexible structures it is natural to investigate ways of adding damping to the structure. One possibility is to use a feedback controller, as demonstrated in Figure 1.

0-7803-9568-9/05/$20.00 ©2005 IEEE

III. Positive position feedback control

For a system of the form (1), a positive position feedback controller is defined as

$$K_{pp}(s) = \sum_{i=1}^{\tilde{N}} \frac{-\gamma_i \gamma_i'}{s^2 + 2\delta_i \tilde{\omega}_i s + \tilde{\omega}_i^2} \tag{3}$$

where $\gamma_i \in \mathbf{R}^{m\times 1}$ for $i = 1, 2, \ldots, \tilde{N}$.

As illustrated in Figure 1, due to the existence of the negative sign in all terms of (3) the overall system resembles a positive feedback loop. Also, the transfer function matrix (1) is similar to that of the force to displacement transfer function matrix associated with a flexible structure, hence the terminology positive position feedback.

An important property of PPF controllers is that to suppress one vibration mode requires only one second order term, as articulated in (3). Consequently, one can choose the modes, within a specific badwidth, that are to be controlled and construct the necessary controller. This ensures that dimensions of the controller remain small, which is beneficial when the controller is being implemented. In the experimental part of this paper we will illustrate that despite their simple structure, the PPF controllers are highly efficient in damping structrural vibrations and are capable of maintaining performance in presence of uncertainty in the structural dynamics of the system.

To derive stability conditions for this control loop, the series in (1) is first truncated by keeping the first N modes ($N < M$) that lie within the bandwidth of interest, and then incorporating the effect of truncated modes by adding a feed-through term to the truncated model. That is to approximate (1) by

$$G^N(s) = \sum_{i=1}^{N} \frac{\psi_i \psi_i'}{s^2 + 2\zeta_i \omega_i s + \omega_i^2} + D. \tag{4}$$

Addition of this feed-through term to the truncated model is quite important, if the truncation is not to substantially alter open-loop zeros of the system. Although the truncation does not perturb open-loop poles of the system, it has the potential to significantly move the open-loop zeros, particularly when the actuators and sensors are collocated. Consequently, if a feedback controller is designed for the truncated model, and then implemented on the real system, the performance and stability of the closed loop system could be adversely affected. This issue has been well-known to the aeroelasticity community and has been referred to as the mode acceleration method [2].

Presently available PPF techniques do not allow for a feed-through term in the plant model. In our experience, however, it is essential to include this in the design phase, if the implemented controller is to perform in a satisfactory manner. Closed-loop performance of a controlled system is highly dependent on open-loop zeros of the plant [11]. Inclusion of a feed-through term in the model ensures that closed-loop performance of the controller, once implemented, is in close agreement with theoretical predictions.

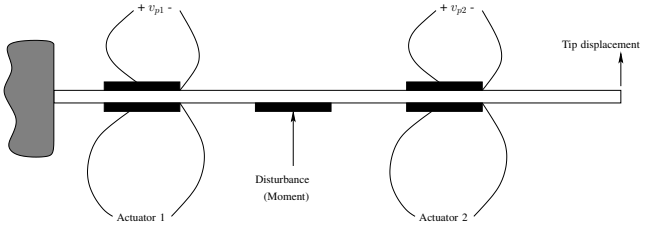

Fig. 2. Beam layout as used in the experiments

The following theorem gives the necessary and sufficient conditions for closed loop stability under positive position feedback. A proof will be given in a more complete version of this paper. First, we need to make the following definitions:

$$\begin{aligned} Z &= diag(\zeta_1, \zeta_2, \ldots, \zeta_N); \quad \Omega = diag(\omega_1, \omega_2, \ldots, \omega_N) \\ \Psi &= \begin{bmatrix} \psi_1 & \psi_2 & \ldots & \psi_N \end{bmatrix}; \quad \Delta = diag(\delta_1, \delta_2, \ldots, \delta_N) \\ \tilde{\Omega} &= diag(\tilde{\omega}_1, \tilde{\omega}_2, \ldots, \tilde{\omega}_N); \quad \Gamma = \begin{bmatrix} \gamma_1 & \gamma_2 & \ldots & \gamma_{\tilde{N}} \end{bmatrix}. \end{aligned}$$

Theorem 1: The negative feedback connection of (4) and (3) with $\Delta > 0$ is exponentially stable if and only if

$$\tilde{\Omega}^2 - \Gamma' D \Gamma > 0 \tag{5}$$

and

$$\Omega^2 - \Psi' \Gamma (\tilde{\Omega}^2 - \Gamma' D \Gamma)^{-1} \Gamma' \Psi > 0. \tag{6}$$

Proof: A proof will be given in the full version of this paper. ■

Therefore, the set of positive position feedback controllers is a convex set characterized by the linear matrix inequalities $\Delta > 0$ and

$$\begin{bmatrix} \Omega^2 & -\Psi'\Gamma & 0 \\ -\Gamma'\Psi & \tilde{\Omega}^2 & \Gamma' \\ 0 & \Gamma & D^{-1} \end{bmatrix} > 0 \tag{7}$$

IV. Experimental setup

All discussions so far were based on analytic models (1), (2) and (4). The model structure of the PPF controller, see (3), strongly resembles the system model structures (1), (2) and (4). Here, a Cantilever beam representing a physical resonant system is considered. This beam, which is clamped at one end and free at the other end, is susceptible to high amplitude vibrations when disturbed. In what follows, a PPF controller will be designed to damp these high amplitude vibrations in the beam. It is worth noting that the cantilever beams of the type to be used here are known to have models of the form (1), (2) and (4), see [9], and resonant controllers designed for them are known to have damped the vibrations to a reasonable extent, see [13] and [10].

In this section a description of the experimental setup meant for both modeling and control of the beam is presented. This setup will remain the same for all the experiments to be performed on the beam.

As mentioned above the cantilever beam is clamped at one end and free at the other. Two pairs of piezoelectric

patches are attached to this beam, one pair located close to the clamped end and the other pair located close to the free end of the beam. For each pair, one piezoelectric patch will be used as an actuator (where input signals are applied) and another patch will act as a sensor (where output signals are recorded). Another solitary piezoelectric patch is attached to the center of the beam and will be driven by a voltage source w. This voltage w represents the

V. System identification

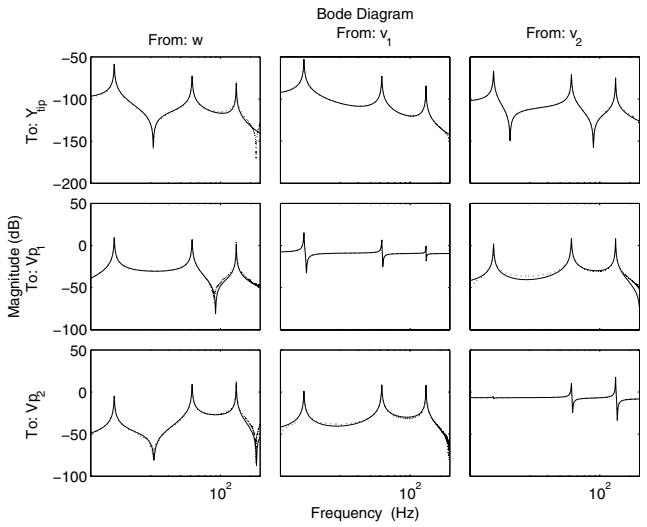

Fig. 3. Identified model (solid) with measured data (dotted)

In order to obtain models for the beam, the experimental setup is treated as a three-input-three-output multivariable system with inputs v_1 and v_2, the voltages applied to the actuators of the collocated piezo patches and the outputs v_{p1} and v_{p2} the voltages induced at the corresponding sensors. The third input w is the disturbance on the beam and the output y_{tip} is the displacement of the the tip of the beam. To be precise, y_{tip} is the displacement of the top vertex point of the beam at the free end.

Since the system is modeled as a three-input-three-output system, the frequency response function (FRF) $G(\mathrm{i}\omega)$ is a 3×3 matrix with each element $G_{ij}(\mathrm{i}\omega), i, j = 1, 2$ and 3, corresponding to a particular combination of the input and the output *i.e.,* $G_{ij}(\mathrm{i}\omega) = G_{y_i u_j} = Y_i(\mathrm{i}\omega)/U_j(\mathrm{i}\omega)$, where $y_1 = y_{tip},\ y_2 = v_{p1}$ and $y_3 = v_{p2}$, and $u_1 = w,\ u_2 = v_1$ and $u_3 = v_2$. $Y_i(\mathrm{i}\omega)$ and $U_j(\mathrm{i}\omega)$ are the Fourier transforms of y_i and u_j respectively. These FRFs are determined (non-parametrically) by applying a sinusoidal chirp of varying frequency (from $5 - 250$Hz) to the piezoelectric actuators (including the central patch corresponding to disturbance term w) and measuring the corresponding output signals y_{tip}, v_{p1} and v_{p2}. The inputs are generated using a standard HP signal generator and the output signals y_{tip}, v_{p1} and v_{p2} were measured using a Polytec laser scanning vibrometer (PSV-300). The vibrometer PSV-300 also includes a software which processes the input output data to give a non-parametric $G(\mathrm{i}\omega)$. A non-parametric $G(\mathrm{i}\omega)$ refers to the case where values of $G(\mathrm{i}\omega)$ are calculated at certain frequency points $\omega_k,\ k = 1, 2, \ldots M$, and interpolated in the intervals $\omega_k \le \omega \le \omega_{k+1}$.

In Figure 3, the non-parametric FRFs $G_{ij}(\mathrm{i}\omega), i, j = 1, 2$ and 3 are plotted. It is apparent from the plots that all the FRFs have three resonance frequencies in the plotted frequency region, and the resonance frequencies are more or less the same for all the FRFs.

The goal here is to have good fits of the form (4) for the collocated FRFs $G_{v_{p1}v_1}$ and $G_{v_{p2}v_2}$, and good fits of the form (2) for all the other FRFs. Past research and our experience with similar systems, see [9] and [13], suggest that the beam in consideration has a multivariable state space model of the form

$$\begin{aligned} \dot{x}(t) &= Ax(t) + B_w w(t) + B_v V(t) && (8)\\ y_{tip} &= C_y x(t) + D_{yw} w(t) + D_{yv} V(t) && (9)\\ V_p(t) &= C_v x(t) + D_{vw} w(t) + D_{vv} V(t), && (10) \end{aligned}$$

where

$$A = \begin{bmatrix} 0 & 1 & & 0 & 0 \\ -\omega_1^2 & -2\zeta_1\omega_1 & & 0 & 0 \\ & & \ddots & & \\ 0 & 0 & & 0 & 1 \\ 0 & 0 & & -\omega_N^2 & -2\zeta_N\omega_N \end{bmatrix} \quad (11)$$

$$B = [B_w \quad B_{v_1} \quad B_{v_2}] = \begin{bmatrix} 0 & 0 & 0 \\ \beta_1 & \Psi_1^{v_1} & \Psi_1^{v_2} \\ \vdots & \vdots & \vdots \\ 0 & 0 & 0 \\ \beta_N & \Psi_N^{v_1} & \Psi_N^{v_2} \end{bmatrix} \quad (12)$$

$$C = \begin{bmatrix} C_y \\ C_{v_1} \\ Cv_2 \end{bmatrix} = \begin{bmatrix} \gamma_1 & 0 & \ldots & \gamma_N & 0 \\ \Psi_1^{v_1} & 0 & \ldots & \Psi_N^{v_1} & 0 \\ \Psi_1^{v_2} & 0 & \ldots & \Psi_N^{v_2} & 0 \end{bmatrix} \quad (13)$$

$$V(t) = \begin{bmatrix} v_1 & v_2 \end{bmatrix}' \quad (14)$$

$$V_p(t) = \begin{bmatrix} v_{p1} & v_{p2} \end{bmatrix}'. \quad (15)$$

The terms D_{yw}, D_{vw}, D_{yv} and D_{vv} are matrices of appropriate diemsnions.

Using Laplace-transforms it can be verified that (8)-(10), enforces the structure (4) on the collocated FRFs $G_{v_{p1}v_1}$ and $G_{v_{p2}v_2}$, and the structure (2) on the other non-collocated FRFs. The model structure (8)-(10) also forces all the FRFs to have the same set of poles.

Note that the given FRF data has only three resonance frequencies, see Figure 3. In other words the given FRF data takes into account only the first three modes of vibrations. The other higher order modes have been discarded (or not taken into account) as they are beyond the frequency regions of interest. Since the given data includes only three modes, it suffices to set $N = 3$, or consider a third order model of the form (8)-(10). A standard method to determine the model parameters $\{\Psi_k^{v_1}, \Psi_k^{v_2}, \beta_k, \gamma_k, \omega_k, \zeta_k\}_{k=1}^N$ and the feed-through terms D_{yw}, D_{yv}, D_{vw} and D_{vv} is to choose

them as the minimizers of the cost function,

$$\mathcal{M} = \sum_{i,j=1}^{3}\sum_{k=1}^{M}\left|\frac{G_{ij}^{N}(\mathrm{i}\omega_k)-G_{ij}(\mathrm{i}\omega_k)}{G_{ij}(\mathrm{i}\omega_k)}\right|^2, \quad (16)$$

where $G_{ij}^{N}(\mathrm{i}\omega)$ are the FRFs corresponding to the multivariable state space model (8)-(10) and ω_k denotes the frequency points where the non-parametric FRFs $G_{ij}(\mathrm{i}\omega)$ are measured.

Minimizing the cost function $\mathcal{M}$, (16), involves using a computationally complex non-linear search. Due to the enormity in the number of parameters to be estimated, the cost function $\mathcal{M}$ may have numerous local minimas. Therefore a poor initial guess for the parameters $\{\Psi_k^{v_1}, \Psi_k^{v_2}, \beta_k, \gamma_k, \omega_k, \zeta_k\}_{k=1}^{N}$, D_{yw}, D_{yv}, D_{vw} and D_{vv} (*i.e.,* parameter values which give poor fits for the FRF data), the non-linear search may land in a local minima which also gives a poor fit for the FRF data. An initialization which in itself gives a decent fit to the FRF data would lead the non-linear search to the parameter values that give a good fit for the FRF data. Though such an initialization seems to be too much of an asking, it is still possible. One approach to get such initial values is to fit the non-parametric data first using subspace methods, [8]. Using subspace methods one can obtain a multivariable state space model, of the same dimensions as (8)-(10), for the FRFs $G_{ij}(\mathrm{i}\omega)$. Even though subspace methods are essentially black box methods, not conforming to any particular model structure, as the cantilever beam is known to posses a model of the form (8)-(10), the subspace fit would also resemble the models (8)-(10) to a large extent. From the subspace fit one can then extract good initial estimates for parameters $\{\Psi_k^{v_1}, \Psi_k^{v_2}, \beta_k, \gamma_k, \omega_k, \zeta_k\}_{k=1}^{N}, D_{yw}, D_{yv}, D_{vw}$ and D_{vv}. Details on using subspace methods have not been presented here as it is very long and laborious. Interested readers are referred to [13] or [8].

In Figure 3 the parametric model, of the form (8)-(10), estimated from the non-parametric FRF data is plotted along with the measured non-parametric FRFs $G_{ij}(\mathrm{i}\omega)$. It is apparent from the plots that the estimated parametric model gives a good fit for the non-parametric data.

VI. PPF CONTROLLER DESIGN

The tip displacement y_{tip} of the beam gives a measure of the amplitude of vibrations in the beam. As w represents disturbance, the FRF $G_{y_{tip}w}(\mathrm{i}\omega) = Y_{tip}(\mathrm{i}\omega)/W(\mathrm{i}\omega)$ is a good indicator of the effect of noise on the beam. A well damped FRF $G_{y_{tip}w}(\mathrm{i}\omega)$ would imply a well damped system. Hence, here, a controller is designed such that the closed loop FRF $G_{Cl,yw}(\mathrm{i}\omega)$ corresponding to the input w and output y_{tip} is well damped. Alternatively stated, a controller is designed such that the poles of the closed loop FRF $G_{Cl,yw}(\mathrm{i}\omega)$ are well inside the left half plane.

The PPF controller to be designed is a two-input two-output multivariable controller, which forms a feedback loop connecting the outputs $V_p(t) = [v_{p1} \;\; v_{p2}]'$ to the inputs $V(t) = [v_1 \;\; v_2]'$ of the system. Sticking to the notations in Section III the PPF controller to be designed is of the form

$$\dot{\tilde{x}}(t) = \tilde{A}\tilde{x}(t) + \tilde{\Gamma}V_p(t) \quad (17)$$

$$V(t) = \tilde{\Gamma}\tilde{x}(t) \quad (18)$$

where

$$\tilde{A} = \begin{bmatrix} 0 & 1 & & 0 & 0 \\ -\tilde{\omega}_1^2 & -2\delta_1\tilde{\omega}_1 & & 0 & 0 \\ & & \ddots & & \\ 0 & 0 & & 0 & 1 \\ 0 & 0 & & -\tilde{\omega}_3^2 & -2\delta_3\tilde{\omega}_3 \end{bmatrix} \quad (19)$$

and

$$\tilde{\Gamma} = \begin{bmatrix} 0 & 0 \\ \Gamma_1^{v_{p1}} & \Gamma_1^{v_{p2}} \\ \vdots & \vdots \\ 0 & 0 \\ \Gamma_3^{v_{p1}} & \Gamma_3^{v_{p2}} \end{bmatrix}. \quad (20)$$

Using (17)-(18) in (8)-(10), the closed loop system can be written in the form

$$\dot{X} = \bar{A}(\tilde{\Omega}, \Delta, \Gamma)X + \bar{B}_w w(t) \quad (21)$$

$$y_{tip} = \bar{C}(\Gamma)X + \bar{D}_{yw}w(t), \quad (22)$$

where $X = [x' \;\; \tilde{x}']'$ and

$$\Gamma = \begin{bmatrix} \Gamma_1^{v_{p1}} & \Gamma_2^{v_{p1}} & \Gamma_3^{v_{p1}} \\ \Gamma_1^{v_{p2}} & \Gamma_2^{v_{p2}} & \Gamma_3^{v_{p2}} \end{bmatrix}. \quad (23)$$

Derivations of the expressions for $\bar{A}(\tilde{\Omega}, \Delta, \Gamma), \bar{B}, \bar{C}$ and $\bar{D}_{yw}$ from (17)-(18) and (8)-(10) involve standard (and straight-forward) calculations, and hence, are omitted here.

The FRF $G_{Cl,yw}(\mathrm{i}\omega)$ corresponding to the closed loop system (21)-(22) is the one that is to be damped by appropriately choosing $\tilde{\Omega}, \Delta$ and Γ. A sufficiency condition for the stability of the closed loop (21)-(22) is provided in Section III, which states that for the closed-loop system $G_{Cl,yw}(\mathrm{i}\omega)$ to be stable the LMI condition (7) has to be satisfied. Hence the PPF controller design problem can be posed as a constrained optimization problem:

$$\min_{\tilde{\Omega},\Delta,\Gamma} \parallel G_{Cl,yw}(\mathrm{i}\omega) \parallel \quad (24)$$

subject to the constraint (7) where

$$\Psi = \begin{bmatrix} \Psi_1^{v_1} & \Psi_2^{v_1} & \Psi_3^{v_1} \\ \Psi_1^{v_2} & \Psi_2^{v_2} & \Psi_3^{v_2} \end{bmatrix}, \quad (25)$$

Ω is the 3×3 diagonal matrix with resonance frequencies of the beam as its diagonal elements, and D denotes the feed-through term D_{vv} of the model, see (10). The design variables Γ, Δ and $\tilde{\Omega}$ are 2×3, 3×3 and 3×3 matrices respectively, with Γ as defined in (23) and the matrices Δ and $\tilde{\Omega}$ being diagonal. In (24) $\parallel \cdot \parallel$ denotes a norm. Here the H_∞ and H_2 norms are used as performance measures. Optimal H_2 and H_∞ PPF controller have been designed and tested, but are not reported here due to limited space.

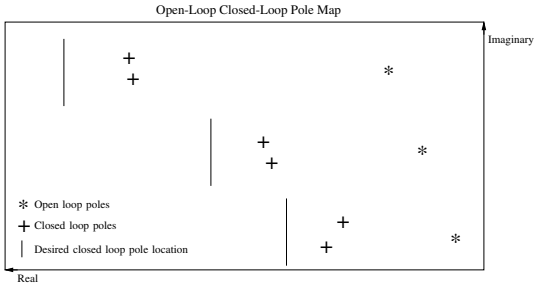

Fig. 4. Pole optimisation procedure

Another alternative, and a more intuitive approach to designing the PPF controller is to place the real parts of the poles of $G_{Cl,yw}(\mathrm{i}\omega)$ as close as possible to a set of desired real values in the left half plane (as shown in Figure 4). In other words choose parameters (Ω, Δ, Γ) such that

$$V = \sum_{k=1}^{N} \mid P_k^d - Re(P_k^c) \mid \tag{26}$$

is minimal under the constraint (7). In (26), P_k^ds denote the prespecified desired set of real values, P_k^c's denote the poles of $G_{Cl,yw}(\mathrm{i}\omega)$ and $Re(\cdot)$ denotes the real part of a complex number. We refer to this optimization approach as the pole optimization approach. In an ideal scenario, one would like the pole optimization approach to provide parameter values (Ω, Δ, Γ) such that $P_k^d = Re(P_k^c)$ for all k.

As in the case of identification, both optimization problems (24) and (26) involve using a non-linear search, which needs to be initialized amicably. One way to initialize the non-linear search would be to solve the LMI (7) using well known LMI solvers like SeDuMi, or Matlab LMI tool box, to obtain a feasible solution. Although such an initial condition would be valid, its use may result in a controller gain $\parallel \Gamma\Gamma' \parallel$ which is too large. A prohibitively large controller gain may result in implementation difficulties. A simple way to obtain initial values is to solve for Γ by solving the LMI (7) for certain fixed values of $\tilde{\Omega}$ and Δ. Past research (see [12], [3] and [4]) and experience with PPF controllers suggest that good PPF designs have their resonance frequencies $\tilde{\Omega}$ close to the system resonance frequencies Ω. Taking this cue, we let

$$\tilde{\Omega} = \kappa\Omega \tag{27}$$

$$\Delta = \frac{\eta}{\kappa}, \tag{28}$$

where κ is scalar reasonably close to one (for example $\kappa = \sqrt{2}$), as our initial guesses for $\tilde{\Omega}$ and Δ. Using the initial values (27) and (28) a meaningful initial guess for Γ can be obtained in the following fashion: Let $\Psi_\perp^{v_1}$ and $\Psi_\perp^{v_2}$ denote vectors orthonormal to $\Psi^1 = [\Psi_1^{v_1} \quad \Psi_1^{v_2}]'$ and $\Psi^2 = [\Psi_2^{v_1} \quad \Psi_2^{v_2}]'$, see (25). Note that due the linear independence of Ψ^1 and Ψ^2 (which is assumed) there exists C_1 and C_2 such that $\Psi^3 = [\Psi_3^{v_1} \quad \Psi_3^{v_2}]'$ is equal to $C_1\Psi^1 + C_2\Psi^2$. Let $\tilde{\Gamma}_C = \begin{bmatrix}\alpha_1\Psi_\perp^1 & \alpha_2\Psi_\perp^2 & 0\end{bmatrix}$, where α_1 and α_2 are real valued parameters, denote a candidate Γ for the initial value. It is easy to note that

$$\Psi'\Gamma_C = \begin{bmatrix} \alpha_1 & 0 & 0 \\ 0 & \alpha_2 & 0 \\ C_1\alpha_1 & C_2\alpha_2 & 0 \end{bmatrix}. \tag{29}$$

Since the feed thorough term D_{vv} is in general very small, we drop the quadratic term $\Gamma' D\Gamma$ in (6) and approximate it by

$$\Omega^2 - \Psi'\Gamma_C\tilde{\Omega}^{-2}\Gamma_C'\Psi > 0. \tag{30}$$

Due to the chosen structure of Γ_C, (30) can be further simplified to

$$\Omega^2\tilde{\Omega}^2 > M'M, \tag{31}$$

where

$$M = \begin{bmatrix} \alpha_1 & 0 & 0 \\ 0 & \alpha_2 & 0 \\ C_1\alpha_1\frac{\tilde{\Omega}_3}{\Omega_1} & C_2\alpha_2\frac{\tilde{\Omega}_3}{\Omega_2} & 0 \end{bmatrix}. \tag{32}$$

Note that the right hand side of (31) is a constant diagonal matrix, therefore choosing α_1 and α_2 such that the bound (31) is satisfied would give an initial guess for Γ_C. However it must be stressed that the approximation introduced in (30) could fail for large values of α_1 and α_2. Hence, it is worth checking if the LMI (6) is satisfied for the chosen initial guesses.

A. Results of pole placement controller design

In this subsection, the results pertaining to the effectiveness of the pole optimized PPF controller are presented.

The controller was designed, and simulations were performed, in a MATLAB/SIMULINK environment. The multivariable controller was then downloaded onto a dSPACE DS-1103 rapid prototyping system. Sampling frequency of the DSP system was set to 20 KHz, and low-pass antialiasing and reconstruction filters with cut-off frequencies of 10 KHz were added to the system. Voltages induced in the two piezoelectric sensors were measured through high-input-impedance buffer circuits, to reduce the low-frquency distortions caused by the finite impedance of the measurement device.

To determine a controller, the desired real parts of closed-loop poles in (26) were placed at -8, -66 and -120 respectively. The real parts of the actual closed-loop poles were found to be -9.7494, -60.8264 and -105.9135 respectively.

To evaluate the damping introduced in the system due to the PPF controller, both the open-loop and the closed-loop FRFs $G_{y_{tip}w}(\mathrm{i}\omega)$ and $G_{Cl,y_{tip}w}(\mathrm{i}\omega)$ are plotted in Figure 5. In this figure experimentally determined $G_{y_{tip}w}(\mathrm{i}\omega)$ and $G_{Cl,y_{tip}w}(\mathrm{i}\omega)$ are plotted. Experimentally determined FRFs refer to the case where the piezoelectric patch corresponding disturbance input w in the cantilever beam setup is driven by a chirp signal and the corresponding output y_{tip} is recorded for both the closed- and the open-loop systems. The FRFs $G_{y_{tip}w}(\mathrm{i}\omega)$ and $G_{Cl,y_{tip}w}(\mathrm{i}\omega)$ are then calculated from the recorded input-output data, as done in the non-parametric

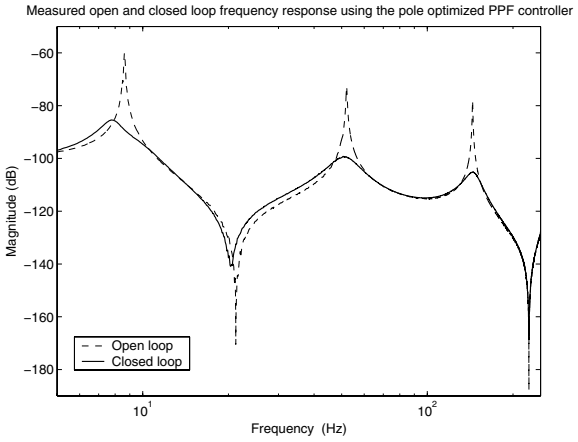

Fig. 5. Measured open- and closed-loop frequency response using the pole optimization

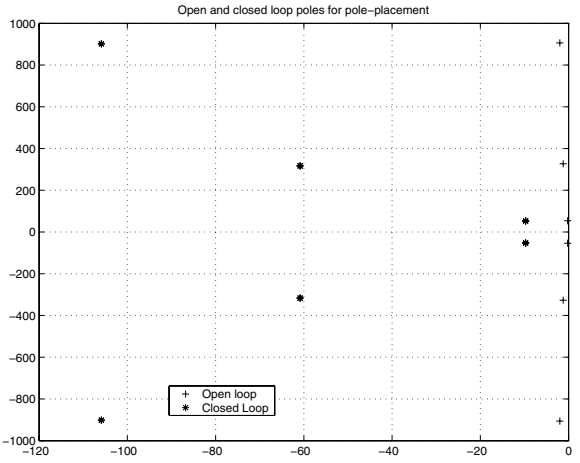

Fig. 6. Open- and closed-loop pole map for the pole placement optimization

identification. The simulation plots and the experimental plots are fairly similar, with the differences being not too noticeable[1]. Thus validating the use of the model (8)-(10) for the beam. The plots also suggest a satisfactory damping in the magnitude of the closed-loop FRF $G_{Cl,y_{tip}w}(\mathrm{i}\omega)$ at the resonance frequencies.

In Figure 6 the open loop poles and the closed loop pole are plotted. It is evident that $G_{Cl,y_{tip}w}(\mathrm{i}\omega)$ is much better damped.

In practice, due to wear and tear and also due to other factors such as surrounding temperature, etc. the material properties of the structure and the piezoelectric patches tend to change. This leads to shifts in the resonance frequencies of the beam. A good controller design must be robust enough to provide good damping even under the changed circumstances. In order to check the robustness of the PPF design, here, artificial shifts in the resonance frequencies of the beam were brought about by adding an extra mass at the

[1]Simulation plots are not included here due to the lack of space.

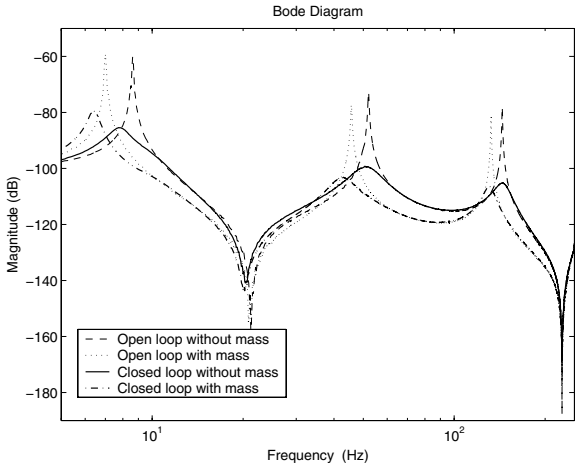

Fig. 7. Measured open- and closed-loop frequency responses using the pole optimization, with and without the mass

free end of the beam. In Figure 7 the measured open-loop and the closed-loop FRFs $G_{y_{tip}w}(\mathrm{i}\omega)$ and $G_{Cl,y_{tip}w}(\mathrm{i}\omega)$ for the loaded system are plotted. It must be stressed that, the PPF controller used in the closed-loop system is the same PPF controller that was used for the unloaded Cantilever beam. The plots suggest that the PPF controller designed using pole optimization is robust with respect to shifts in the resonance frequencies.

REFERENCES

[1] M. J. Balas. Active control of flexible systems. *Journal of Optimization Theory ans Applications*, 25(3):415–436, 1978.

[2] R. L. Bisplinghoff and H. Ashley. *Principles of Aeroelasticity*. Dover Publications Inc., 1962.

[3] J. L. Fanson and T. K. Caughey. Positive position feedback control for large space strcture. In *Proc. 28th AIAA/ASME/ASC/AHS Structures Structural Dynamics and Materials Conference*, pages 588–598, Monterey, California, 1987.

[4] J. L. Fanson and T. K. Caughey. Positive position feedback-control for large space structures. *AIAA Journal*, 28(4):717–724, April 1990.

[5] C. J. Goh and T. K. Caughey. On the stability problem caused by finite actuator dynamics in the collocated control of large space structures. *International Journal of Control*, 41(3):787–802, 1985.

[6] J. Juang and M. Q. Phan. *Identification and Control of Mechanical Systems*. Cambridge University Press, 2001.

[7] G. D. Martin. *On the control of flexible mechanical systems*. PhD thesis, Stanford University, 1978.

[8] T. McKelvey, H. Ackay, and L. Ljung. Subspace-based identification of infinite-dimensional multi-variable systems from frequency-response data. *IEEE Transactions on Automatic Control*, AC–41:960–979, 1996.

[9] S. O. R. Moheimani, D. Halim, and A. J. Fleming. *Spatial Control of Vibration: Theory and Experiments*. World Scientific, Singapore, 2003. ISBN: 981-238-337-9.

[10] S. O. R. Moheimani and B. J. G. Vautier. Resonant control of structural vibration using charge-driven piezoelectric actuators. In *Proc. IEEE Conference on Decision and Control*, Bahamas, 2004.

[11] M. M. Seron, J. H. Braslavsky, and G. C. Goodwin. *Fundamental Limitations in Filtering and Control*. Springer, London, 1997.

[12] G. Song, S. P. Schmidt, and B. N. Agrawal. Experimental robustness study of positive position feedback control for active vibration suppression. *Journal of Guidance, Control and Dynamics*, 25(1):179–182, 2002.

[13] B. J. G. Vautier. Charge-driven piezoelectric actuators in structural vibration control applications. Master's thesis, The University of Newcastle, 2004.